Journal of ELECTRICAL ENGINEERING, VOL. 57, NO. 6, 2006, 305–317

DECENTRALIZED ROBUST AGC BASED ON STRUCTURED SINGULAR VALUES

Hossein Shayeghi [*] — **Heidar Ali Shayanfar** [**]

In this paper, a new approach based on structured singular value (μ-synthesis) is presented for the robust decentralized automatic generation controller design of a deregulated multi area power systems under the possible contracts. In each control area, the connections between this area and the rest of the system and the effects of possible contracts are treated as a set of new disturbance signals to achieve decentralization. It is shown that, subject to a condition based on the structured singular values and H_∞ norm, each local area automatic generation controller can be designed independently. The stability condition for the overall system can be stated as to achieve a sufficient interaction margin and a sufficient gain and phase margin defined in classical feedback theory during each independent design. The proposed method is tested on a four-area power system with the possible contracts and compared with the PI controller for a wide range of operating conditions and load changes. The resulting controllers are shown to minimize the effects of load disturbances and maintain robust performance in the presence of specified uncertainties and system nonlinearities.

K e y w o r d s: AGC, decentralized control, multi machine deregulated power system, μ-synthesis, robust control

1 INTRODUCTION

Currently, the electric power industry is in transition from large, vertical utilities providing power at regulated rates to an industry that will incorporate competitive companies selling unbundled power at lower rates. Under this circumstance, any power system controls such as the Automatic Generation Control (AGC) as an ancillary service acquires a principal role to maintain the electric system reliability at an adequate level and is becoming much more significant today in accordance with the complexity of interconnected power system [1, 2]. The goal of AGC is to re-establish primary frequency regulation capacity, return the frequency to its nominal value and minimize unscheduled tie-line power flows between neighboring control areas. That is why during the past decade several proposed AGC scenarios attempted to adapt well tested traditional AGC schemes to the change of environment in power system operation under deregulation [3–9].

In the dynamical operation of power systems, it is usually important to aim for decentralization of control action to individual areas. This aim should coincide with the requirements for stability and load frequency scheduling within the overall system. In a completely decentralized control scheme, the feedback controls in each area are computed on the basis of measurements taken in that area only. This implies that no interchange of information among areas is necessary for the purpose of load frequency control. The advantages of this operating philosophy are apparent in providing cost savings in data communications and in reducing the scope of the monitoring network.

One of the important issues in the AGC design problem is robustness against uncertainties and disturbances. On the other hand, in the restructured power system increasing size and complexity of the interconnected power system introduced a set of significant uncertainties and disturbances in power system control and operation, especially on the AGC problem solution. Thus, it is desirable that the novel control strategies be developed to achieve AGC goals and maintain reliability of the electric power system in an adequate level. There have been continuing efforts in design of load frequency controller with better performance according to the change of environment in power system operation under deregulation using various optimal and robust control strategies during the recent years [10–13]. The proposed methods gave good dynamical responses, but robustness in the presence of large modelling uncertainties was not considered and stability of the overall system was not guaranteed. Also, some of them have a centralized scheme which is not feasible for a large power system because of computational and economical difficulties in implementing this scheme.

One of the most important in control theory and application was the direct and inverse Nyquist array methods developed by Rosenbrock and his colleagues [14–16]. The design is based on achieving the required diagonal dominance, so that each control loop can be designed independently. However, it has long been recognized that the main difficulty in applying the Nyquist array method is to obtain the required diagonal dominance (row dominance or column dominance). In particular, if the controller is restricted to be diagonal, the possibility of achieving diagonal dominance depends on whether the P-F (Perron-Frobenius) eigenvalues of all the matrices derived from

[*] Technical Eng. Dept., The University of Mohaghegh, Ardebili, Iran. E-mail: h_shayeghi@yahoo.com

[**] Electrical Eng. Dept., IUST, Narmak, Tehran 16844, Iran. Email: hashayanfar@yahoo.com

ISSN 1335-3632

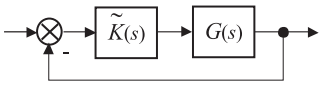

Fig. 1. An equivalent MIMO system.

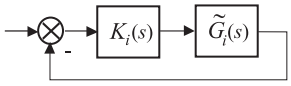

Fig. 2. Independent SISO system design.

the frequency response magnitudes are less than 2 [15, 17]. As shown in Sec. 5, for the sample system studied in this paper, the above P-F eigenvalue condition is not satisfied.

In this paper to break the limit imposed by the diagonal dominance, the problem of decentralized load frequency controller design is translated into an equivalent problem of decentralized controller design for a Multi-Input Multi-Output (MIMO) control system. It is shown that subject to a condition based on the H_∞ norm and structured singular values (μ), each local area controller can be designed independently such that stability of the overall closed loop system is guaranteed. The robust stability condition for the overall system can be easily stated as to achieve a sufficient interaction margin, and a sufficient gain and phase margins during each independent design. Based on this framework, a new local automatic generation controller is designed for satisfying system performances based on μ-synthesis technique using the modified traditional dynamical model for the AGC scheme according to the possible load following contracts. To achieve decentralization, the effects of possible contracted scenarios and connections between each area with the rest of system are treated as a set of new input disturbance signals in each control area. The motivation of using this control strategy is flexibility of the synthesis procedure for modelling uncertainty, direct formulation of performance objectives and practical constraints. Due to its practical merit, the proposed μ-based controller has a decentralized scheme and requires only the Area Control Error (ACE). When a decentralized AGC is applied, by reducing the system size the resulting controller order will be lower, which is ideally useful for the real world complex power systems. The proposed control strategy is applied to a four-area deregulated example. The results are compared with the conventional PI controller, which is widely used in practical industry, for three scenarios of the possible contracts under large load changes in the presence of parametric uncertainties and system nonlinearities.

This paper is organized as follows. Decentralized control design is given in Sec. 2. The generalized dynamic model of AGC scheme in a deregulated electricity market is presented in Sec. 3. Sec. 4 describes the problem formulation for a given control area based on μ-synthesis technique. The proposed strategy is applied to a four-area power system as a case study in Sec. 5. In Sec. 6, some simulation results are given to illustrate robustness of the proposed controllers. Finally, the conclusions are presented in Sec. 7.

2 DECENTRALIZED CONTROLLER DESIGN

A centralized controller design is often considered not feasible for large-scale systems such as power system; in turn decentralized control is adopted. The advantages of a decentralized controller design are reduction in the controller complexity and suitability for practical implementation. In the next subsections, the problem of decentralized automatic generation controller is translated into an equivalent problem of decentralized control design for a MIMO control system. The proposed method is based on the H_∞ norm and structured singular value (μ).

2.1 Problem formulation

In general, an N-area power system AGC problem can be modelled as a large-scale power system consisting of N subsystems:

$$\begin{aligned} \dot{x} &= A_N x + B_N u \\ y &= C_N x \end{aligned} \tag{1}$$

where $u = [u_1, \ldots, u_N]^\top$; $y = [y1, \ldots, y_N]^\top \mathrm{T}$; $x = [x_1, \ldots, x_N]^\top$ and x_i are the state variables for the ith area. Equivalently, this system composed of N linear time-invariant subsystem $G_i(s)$, described by:

$$\begin{aligned} \dot{x}_i &= A_{ii} x_i + \sum_{\substack{j=1 \\ j \neq i}}^{N} A_{ij} x_j + B_{ii} u_i \\ y_i &= C_{ii} x_i \end{aligned} \tag{2}$$

It assume that all (A_{ii}, B_{ii}) are controllable, (A_{ii}, C_{ii}) are observable and all A_{ii} and C_{ii} are full rank. The term $\sum_{\substack{j=1 \\ j \neq i}}^{N} A_{ij} x_j$ is due to the interconnections other subsystems. An $N \times N$ transfer function matrix $G(s)$ linking $U(s)=[u_1(s), \ldots, u_N(s)]^\top$ and $Y(s)=[y_1(s), \ldots, y_N(s)]^\top$:

$$Y(s) = G(s)U(s) \tag{3}$$

can be calculated as:

$$G(s) = C_N(sI - A_N)^{-1} B_N \,. \tag{4}$$

The design of N decentralized local controllers now becomes the design of an $N \times N$ diagonal matrix $\widetilde{K}(s) = \mathrm{diag}\{K_i(s)\}_{i=1,\ldots,N}$ as shown in Figs. 1 and 2.

If all A_{ij} $(i \neq j)$ in $G_i(s)$ were equal to zero, then each controller could be designed by independently just as if it were in a SISO system as shown in Fig. 2. However, since A_{ij} $(i \neq j)$ are not zeros, the following question must be resolved, *ie* if each $K_i(s)$ $(i = 1, \ldots, N)$ is designed to form a stable closed loop system as shown in Fig. 2, what are the additional conditions which can guarantee that the overall system of Fig. 1 is stable? The answer to this question is discussed in the next subsection based on the theorem given by Labibi and *et al* [18].

2.3 Stability condition

In Labibi's paper, $\widetilde{G}(s)$ is considered as the matrix consisting of the diagonal elements of $G(s)$; *ie*:

$$\begin{aligned}\widetilde{G}(s)&=\mathrm{diag}\{\widetilde{G}_i(s)\}=\\&=\mathrm{diag}\{\widetilde{G}_1(s),\widetilde{G}_2(s),\ldots,\widetilde{G}_N(s)\}\end{aligned} \tag{5}$$

where $\widetilde{G}_i(s)$ is the ith diagonal element of the transfer function matrix $G(s)$ and has the following state-space realization:

$$\begin{aligned}\dot{x}_i &= A_{ii}x_i + B_{ii}u_i\\ y_i &= C_{ii}x_i\end{aligned} \tag{6}$$

Using the notations:

$$\begin{aligned}\widetilde{K}(s)&=\mathrm{diag}\{K_i(s)\}=\\&=\mathrm{diag}\{K_1(s),K_2(s),\ldots,K_N(s)\}\end{aligned} \tag{7}$$

$$\widetilde{A} = \mathrm{diag}\{A_{ii}\} = \mathrm{diag}\{A_{11},A_{22},\ldots,A_{NN}\} \tag{8}$$

$$A_d = A - \widetilde{A} \tag{9}$$

Labibi and *et al* have proved the following theorem:

The close loop overall system is stable if:

(c-1) The decentralized controller $\widetilde{K}(s)$ stabilizes the diagonal system $\widetilde{G}(s)$.

(c-2) $\rho_{\max} < \mu^{-1}(A_d)$.

where, $\rho_{\max} = \max\limits_i\{\|(sI-A_{ii}+B_{ii}K_i(s)C_{ii})\|_\infty\}$, $\|\cdot\|_\infty$ is the H_∞ norm and μ denotes Doyle's structured singular value. This theorem gives sufficient conditions for the stability of the overall closed loop system. However, Authors have shown that although (c-2) may has some conservativeness compared the diagonal dominant and the generalized diagonal dominant conditions, it gives the tightest restrictive band and is less conservative than the one proposed by the Grosdidier and Morari [19]. Before applying the above results to our system it is necessary to consider the issue of the robust stability. The stability condition (c-2) is given for the nominal plant $G(s)$. If the state space model of Eq. (1) changes, the plant model of $G(s)$ will also change. It is generally not possible to establish a clear relationship between the change of values in Eq. (1) and the change of values involved in condition (c-2). For this reason, we specify the robust stability conditions as:

(r-1) Condition (c-2) is satisfied with a sufficient margin. This is can be checked by computing $\rho_{\max}$ and $\mu^{-1}(A_d)$ and an Interaction Margin (IM) that can be defined as the difference between values of $\mu^{-1}(A_d)$ and $\rho_{\max}$.

(r-2) There are sufficient gain and phase margins in each SISO loop for the stability. This can also be checked by a Bode or Nyquist plot of $K_i(s)\widetilde{G}_i(s)$.

R e m a r k . For most systems, a satisfactory disturbance rejection performance can be achieved if there are sufficient stability margin.

3 DESCRIPTION OF GENERALIZED AGC SCHEME

In the deregulated power systems, the vertically Integrated Utility (VIU) structure, which supplies power to the customers at regulated rates no longer exists, however, the common AGC objectives, *ie* restoring the frequency and the net inter-changes to their desired values for each control area still remain. Generalized dynamical model or the AGC scheme has been developed in Ref. [6] based on the possible contracts. This section gives a brief overview on this generalized model that uses all the information required in a VIU industry plus the contract data information.

In the deregulated power system, Generation Companies (GENCOs) may or may not participate in the AGC task and Distribution Companies (DISCOs) have the liberty to contract with any available GENCOs in their own or other areas. Thus, there are can be various combinations of possible contract scenarios between DISCOs and GENCOs. The concept of an '*Augmented Generation Participation Matrix*' (AGPM) is introduced to express these possible contracts in the generalized model. The rows and columns of AGPM matrix is equal with total number of GENCOs and DISCOs in the overall power system, respectively. The AGPM structure for a large scale power system with N control area is given by:

$$AGPM = \begin{bmatrix} AGPM_{11} & \ldots & AGPM_{1N}\\ \vdots & \ddots & \vdots\\ AGPM_{N1} & \ldots & AGPM_{NN}\end{bmatrix} \tag{10}$$

where,

$$AGPM_{ij} = \begin{bmatrix} gpf_{(s_i+1)(z_j+1)} & \cdots & gpf_{(s_i+1)(z_j+m_j)}\\ \vdots & \ddots & \vdots\\ gpf_{(s_i+n_i)(z_j+1)} & \cdots & gpf_{(s_i+n_i)(z_j+m_j)}\end{bmatrix}$$

for $i,j=1,\ldots,N$ and $s_i=\sum_{k=1}^{i-1}n_k$, $z_j=\sum_{k=1}^{j-1}m_k$, & $s_1=z_1=0$.

In the above, n_i and m_i are the number of GENCOs and DISCOs in area i and gpf_{ij} refer to '*generation participation factor*' and shows the participation factor GENCO i in total load following requirement of DISCO j based on the possible contracts. The sum of all entries in each column of AGPM is unity.

Block diagram of a generalized AGC scheme for control area i in a deregulated power system is shown in Fig. 3. The nomenclature used is given in Appendix A. the Dashed dot-lines show the connections between each area with the rest of the system and the demand signals based on the possible contracts. These new information signals are considered as disturbance channels for the decentralized AGC design. As there are many GENCOs in each area, ACE signal has to be distributed among them

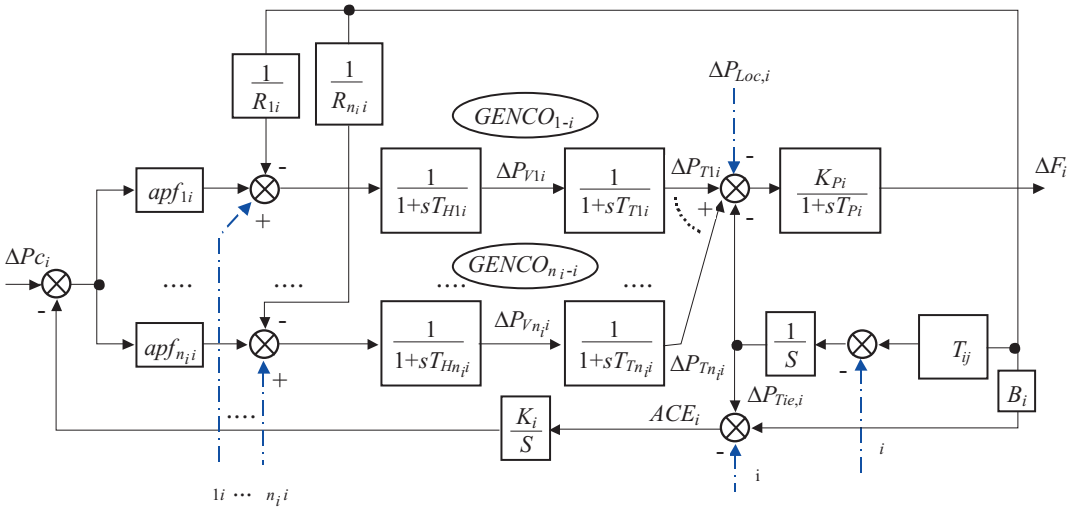

Fig. 3. The generalized AGC scheme for area i in the deregulated environment.

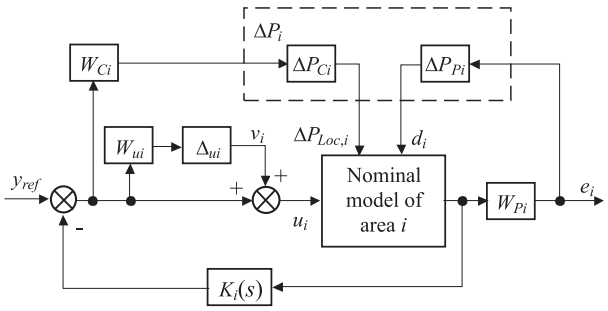

Fig. 4. The proposed synthesis strategy for area i.

due to their ACE participation factor in the AGC task and $\sum_{j=1}^{n_i} apf_{ji} = 1$. We can write [6]:

$$\Delta P_{Loc,i} = \sum_{j=1}^{m_i} \left(\Delta P_{Lj} + \Delta P_{ULj}\right) \tag{11}$$

$$\eta_i = \sum_{\substack{j=1 \\ j\neq i}}^{N} T_{ij} \Delta f_j \tag{12}$$

$$\zeta_i = \Delta P_{tie,i,sch} = \sum_{\substack{k=1 \\ k\neq i}}^{N} \Delta P_{tie,jk,sch} \tag{13}$$

$$\Delta P_{tie,jk,sch} = \sum_{j=1}^{n_i}\sum_{t=1}^{m_k} apf_{(s_i+j)(z_k+t)} \Delta P_{L(z_k+t)} - \sum_{t=1}^{n_k}\sum_{j=1}^{m_i} apf_{(s_k+t)(z_i+j)} \Delta P_{L(z_i+j)} \tag{14}$$

$$\Delta P_{tie,i-error} = \Delta P_{tie,i-actual} - \zeta_i \tag{15}$$

$$\rho_i = [\rho_{1i}, \ldots, \rho_{ki} \ldots, \rho_{n_i i}]^\top,\ \rho_{ki} = \sum_{j=1}^{z_{n+1}} gpf_{(s_i+k)j} \Delta P_{Lj} \tag{16}$$

$$\Delta P_{m,k-i} = \sum_{j=1}^{z_{n+1}} gpf_{(s_i+k)j} \Delta P_{Lj-i} + apf_{ki} \sum_{j=1}^{m_i} \Delta P_{ULj-i} \tag{17}$$

$\Delta P_{m,ki}$ is the desired total power generation of a GENCO k in area i and must track the demand of the DISCOs in contract with it in the steady state.

Due to Fig. 3, the state-space model for control area i can be obtained as:

$$\begin{aligned} \dot{x}_i &= A_i x + B_{iu} u + B_{iw} w_i' \\ y_i &= C_i x_i + + D_{iw} w_i' \end{aligned} \tag{18}$$

where, $x_i^\top = [x_{ai}\ x_{1i}\ \ldots\ x_{ki}\ \ldots\ x_{n_i i}]$, $u_i = \Delta P_{ci}$, $y_i = ACE_i$, $x_{ai} = \left[\Delta f_i\ \Delta tie, i \int ACE_i\right]$, $x_{ki} = [\Delta P_{Tki}\ \Delta P_{Vki}]$, $k = 1, \ldots, n_i$, $w_i'^\top = [\Delta P_{Loc,i}\ \eta_i\ \xi_i\ \rho_i]$,

$$A_i = \begin{bmatrix} A_{11i} & A_{12i} \\ A_{21i} & A_{22i} \end{bmatrix},\ A_{11i} = \begin{bmatrix} 1/T_{Pi} & -K_{Pi}/T_{Pi} & 0 \\ \sum_{\substack{j=1 \\ j\neq i}}^{N} T_{ji} & 0 & 0 \\ B_i & 1 & 0 \end{bmatrix},$$

$$A_{12i} = \underbrace{\left[\begin{pmatrix} K_{Pi}/T_{Pi} & 0 & 0 \\ 0 & 0 & 0 \\ 0 & 0 & 0 \end{pmatrix} \ \ldots\ \begin{pmatrix} K_{Pi}/T_{Pi} & 0 & 0 \\ 0 & 0 & 0 \\ 0 & 0 & 0 \end{pmatrix}\right]}_{n \text{ blocks}},$$

$$A_{21i} = \left[DP_{1i}^\top \ \ldots\ DP_{ki}^\top \ \ldots\ DP_{n_i i}^\top\right],$$

$$A_{22i} = \operatorname{diag}\left(TG_{1i}, \ldots, TG_{ki}, \ldots, TG_{n_i i}\right),$$

$$DP_{ki} = \begin{bmatrix} 0 & 0 & 0 \\ -1/(R_{ki} T_{Hki}) & 0 & -K_i apf_{ki}/T_{Hki} \end{bmatrix},$$

$$TG_{ki} = \begin{bmatrix} -1/T_{Tki} & 1/T_{Tki} \\ 0 & -1/T_{Hki} \end{bmatrix},$$

$$B_{iu}^\top = \left[0_{3\times 1}^\top\ B_{1iu}^\top \ \ldots\ B_{kiu}^\top \ \ldots\ B_{n_i iu}^\top\right],$$

$$B_{kiu} = [0\ \ apf_{ki}/T_{Hki}],$$

$$B_{iw}^\top = \left[B_{aiw}^\top\ B_{1iw}^\top \ \ldots\ B_{kiw}^\top \ \ldots\ B_{n_i iw}^\top\right],$$

$$B_{aiw} = \begin{bmatrix} -K_{pi}/T_{pi} & 0 & 0 & 0_{1\times n_i} \\ 0 & -1 & 0 & 0_{1\times n_i} \\ 0 & 0 & -1 & 0_{1\times n_i} \end{bmatrix},$$

$$B_{kiw} = \begin{bmatrix} 0_{1\times 3} & 0\ \ldots\ 0\ \ldots\ 0 \\ 0_{1\times 3} & b_{1i} \ldots\ b_{ki} \ldots\ b_{n_i i} \end{bmatrix},$$

$$b_{ji} = \begin{cases} 1/T_{Hki} & j = i \\ 0 & j \neq i \end{cases},\ C_i = [C_{ai}\ \ 0_{1\times 2n_i}],$$

$$C_{ai} = [B_i\ \ 1\ \ 0],\ D_{iw} = [0_{1\times 2}\ \ -1\ \ 0_{1\times n_i}].$$

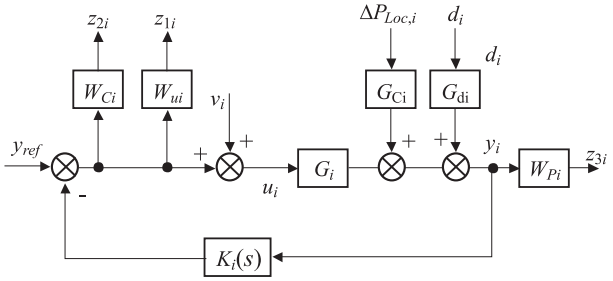

Fig. 5. Synthesis framework for area i.

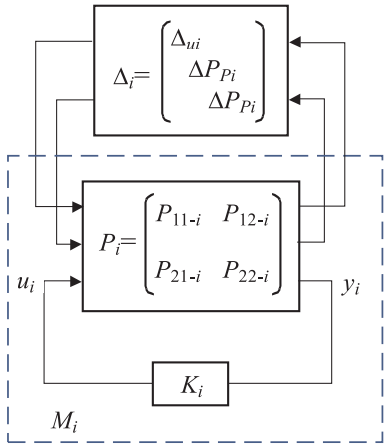

Fig. 6. The standard $M-\Delta$ configuration.

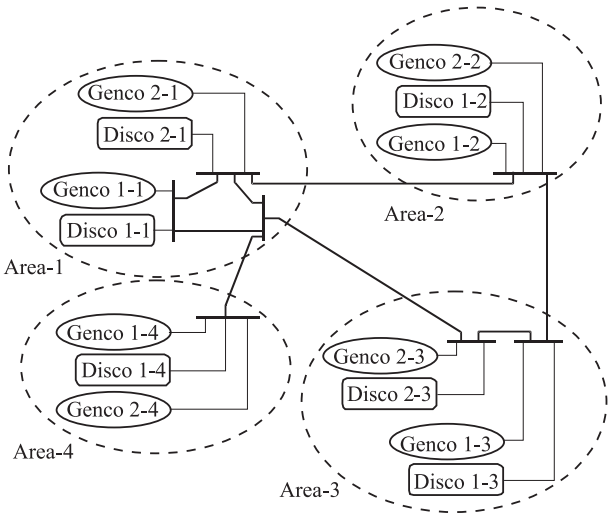

Fig. 7. Four area control power system.

Interested readers can find more detail on the above AGC modelling and simulation for a given deregulated power system in Refs. [6, 20].

4 SYNTHESIS METHODOLOGY

The main goals of the AGC design are: frequency regulation, tracking the load changes and maintaining tie-line power interchanges to specified values in the presence of model uncertainties, system nonlinearities and disturbances. We now proceed to design a decentralized robust controller using the μ-synthesis technique. To achieve our objectives and according to μ-synthesis requirements, we propose the control strategy shown in Fig. 4 for a given control area (Fig. 3). In fact, this figure shows the main synthesis strategy for obtaining the desired decentralized controller.

In the restructured power systems, each control area contains different kinds of uncertainties because of plant parameter variations and load changes due to some approximations in model linearization and un-modelled dynamics. Usually, the uncertainties in power system can be modelled as multiplicative and/or additive uncertainties [21]. However, to keep the complexity of the controllers reasonably low, depending on the given control area, it is better to focus on the most important uncertainties. In Fig. 4 the Δu_i block models the unstructured uncertainties as a multiplicative type and Wu_i is the associated weighting function. According to the requirements of performance and practical constraint on control actions, the weighting functions W_{Ci} and W_{Pi} are added to the control area model. This is necessary in order to guarantee implement ability of the resulting controller. W_{Ci} on the control input sets a limit on the allowed control signal to penalize fast change and large overshoot in the control action. The weight, W_{Pi}, at the output sets the performance goal *ie*: tracking regulation error on the output area control signal. ΔP_{Ci} and ΔP_{Pi} are uncertainty blocks associated with W_{Ci} and W_{Pi}, respectively.

The synthesis starts with setting the desired level of stability and performance for a given control area with a set of (u_i, y_i) and chosen uncertainties to achieve robust performance. The next task is to isolate the uncertainties from the nominal plant model and redraw the system in the standard $M-\Delta$ configuration. We can redraw Fig. 4 as shown in Fig. 5, where G_i, G_{Ci} and G_{di} are transfer functions to the y_i from the control input (u_i) and input disturbances $\left(\Delta P_{Loc,i}, d_i\right)$, respectively and we have:

$$\begin{aligned} d_i^{\top} &= [\eta_i, \zeta_i, \rho_{1i}, \ldots, \rho_{ki}, \ldots, \rho_{n_i i}] \\ G_{d_i} &= \left[G_{\eta_i}, G_{\zeta_i}, G_{\rho_{1i}}, \ldots, G_{\rho_{ki}}, \ldots, G_{\rho_{n_i i}}\right] \\ W_{Pi}^{\top} &= \left[W_{\eta_i}, W_{\zeta_i}, W_{\rho_{1i}}, \ldots, W_{\rho_{ki}}, \ldots, W_{\rho_{n_i i}}\right] \\ z_{3i}^{\top} &= [z_{3i-1}, z_{3i-2}, z_{3i-3}, \ldots, z_{3i-k+2}, \ldots, z_{3i-n_i+2}] \end{aligned} \tag{19}$$

The standard $M-\Delta$ configuration for area i is shown in Fig. 6, where P_i include the nominal plant, the weighting functions and scaling factor. As is mentioned in the above, the blocks ΔP_{Pi} described by:

$$\Delta P_{Pi} = \operatorname{diag}\left(\Delta P_{\eta i}, \Delta P_{\xi i}, \Delta P_{\rho 1 i}, \ldots, \Delta P_{\rho k i}, \ldots, \Delta P_{\rho n_i i}\right) \tag{20}$$

are the fictitious uncertainties added to ensure robust performance, while the block Δ_{ui} models important multiplicative uncertainty associated with the control area model.

Table 1. GENCOs parameter

MVA_{base} (1000MW) Parameter	GENCOs (k in area i)							
	1-1	2-1	1-2	2-2	1-3	2-3	1-4	2-4
Rate (MW)	800	1000	1100	1200	1000	1000	900	1000
T_T (sec)	0.36	0.42	0.44	0.40	0.36	0.40	0.38	0.40
T_H (sec)	0.06	0.07	0.06	0.08	0.07	0.08	0.085	0.08
R (Hz/pu)	2.4	3.3	2.5	2.4	3	2.4	2	2.4
Apf	0.5	0.5	0.6	0.4	0.5	0.5	0.5	0.5

Table 2. Control area parameters

Parameter	Area-1	Area-2	Area-3	Area-4
K_P (Hz/pu)	120	112.5	125	115
T_P (sec)	20	25	20	25
B (pu/Hz)	0.425	0.385	0.359	0.425
K	0.63	1.15	0.89	0.29
T_{ij} (pu/Hz)	$T_{12}=0.219, T_{13}=0.245, T_{14}=0.109, T_{23}=0.175$			

Now, the synthesis problem is designing the robust control $K_i(s)$. Ideally, based on the μ-theory [22], the robust stability and performance holds for a given $M-\Delta$ configuration if and if only:

$$\inf_{K_i} \sup_{\omega} \mu_{\Delta}\big(M_i(j\omega)\big) \leq 1 \tag{21}$$

where according to Fig. 5, block labelled M_i in Fig. 6 for area i is given by:

$$M_i = \begin{bmatrix} W_{ui}T_i & -W_{ui}G_i^{-1}G_{Ci}T_i & W_{ui}G_{di}G_i^{-1}T_i \\ -W_{Ci}T_i & -W_{Ci}G_i^{-1}G_{Ci}T_i & W_{Ci}G_{di}G_i^{-1}T_i \\ W_{Pi}G_iS_i & W_{Pi}G_{Ci}S_i & W_{Pi}G_{di}S_i \end{bmatrix} \tag{22}$$

T_i and S_i are complementary sensitivity and sensitivity functions of the nominal model of control area i and described by:

$$\begin{aligned} T_i &= G_iK_i(1+G_iK_i)^{-1} \\ S_i &= 1-T_i = (1+G_iK_i)^{-1} \end{aligned} \tag{23}$$

In other words, the performance and stability of the closed loop system M_i is a μ test, across frequency for the given uncertainty structure Δ_i. Using the performance robustness condition and the well-known upper bound for μ, the robust synthesis problem is reduced to solve the following problem:

$$\min_{K_i} \inf_{D} \sup_{\omega} \overline{\sigma}\big(DM_i(j\omega)D^{-1}\big) \tag{24}$$

or equivalently:

$$\min_{K_i} \inf_{D} \big\| DF_L(P_i,K_i)D^{-1} \big\|_{\infty} \tag{25}$$

by iteratively, solving for D and K_i ($D-K$ iteration algorithm). Here D is any positive definite symmetric matrix with appropriate dimension and $\overline{\sigma}(\cdot)$ denotes the maximum singular value of a matrix. This problem can be solved using the MATLAB μ-synthesis toolbox [23]. It should be noted that the order resulting controller by this procedure is usually high. In order to decrease the complexity of computation in the case of high order power systems, appropriated model reduction techniques might be applied to the obtained controller model. In summary the synthesis procedures of the proposed strategy are:

Step 1: Formulation of the AGC problem as a decentralized control scheme due to Fig. 3 and identify the state space model for the given control area.

Step 2: Identify the uncertainty blocks and associated weighting functions for the given area as shown in Fig. 4 according to dynamical model, practical limits and performance requirements.

Step 3: Isolate the uncertainties from the nominal area model, generate the Δu_i, ΔP_{Ci} and ΔP_{Pi} blocks and obtaining $M-\Delta$ configuration to formulate the desired level of robust performance.

Step 4: Start $D-K$ iteration algorithm using the μ-synthesis toolbox to obtain the optimal controller.

Step 5: Reduce the order of the resulting controller by using the standard model reduction techniques and apply μ-analysis to the closed loop system with reduced controller to check whether or not the upper bound of μ remains less than one.

Step 6: Continue this procedure by applying the above steps to other control area.

Step 7: Retune the obtained decentralized controller to best performance and check if the overall power system satisfies the robust stability condition as given in Sec. 2 and has enough IM, gain and phase margins.

The proposed control methodology in this paper includes enough flexibility to set the desired level of robust performance and provides a set of robust decentralized controllers which guarantee stability of the overall power system. On the other hand, it has a decentralized scheme and requires only the ACE in each control area. Thus, its construction and implementation are easy and can be useful in the real world complex power systems.

5 CASE STUDY

A four-area power system, shown in Fig. 7 is considered as a test system to demonstrate the effectiveness of the proposed control strategy. It is assumed that each control area includes two GENCOs and two DISCOs except areas two and four have one DISCOs. The power system parameters are given in Tables 1 and 2.

According to problem formulation given in Sec. 2, the state-space realization of the overall system can be constructed as:

$$\begin{aligned} \dot{x} &= Ax + Bu \\ y &= Cx \end{aligned} \tag{26}$$

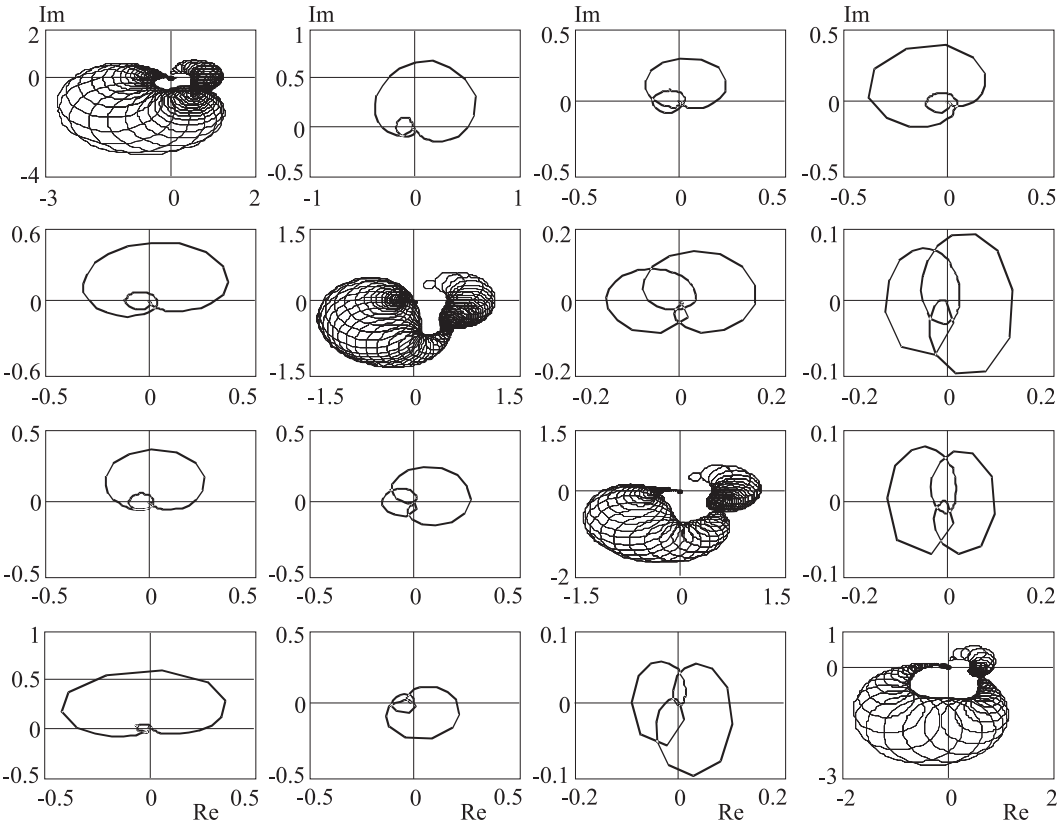

Fig. 8. Nyquist array with the row Gershgorin circles.

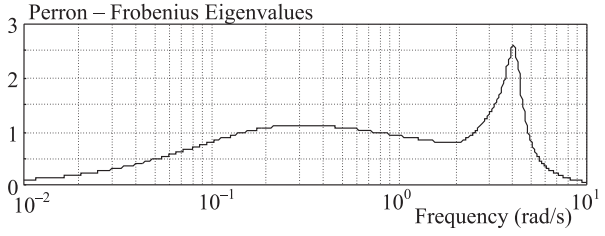

Fig. 9. P-F eigenvalues for the $G(s)$.

where $u = [u_1\ u_2\ u_3\ u_4]^\top$; $y = [y_1\ y_2\ y_3\ y_4]^\top = [ACE_1\ ACE_2\ ACE_3\ ACE_4]^\top$; $x = [x_1\ x_2\ x_3\ x_5]^\top$ and x_i is the state variables for ith area as given in Eq. (18), $A \in R^{28\times 28}$, $B \in R^{28\times 4}$, $C \in R^{4\times 28}$;

$$A = \begin{bmatrix} A_{11} & A_{12} & A_{13} & A_{14} \\ A_{21} & A_{22} & A_{23} & A_{24} \\ A_{31} & A_{32} & A_{33} & A_{34} \\ A_{41} & A_{42} & A_{43} & A_{44} \end{bmatrix},$$

$B = \text{blockdiag}\big(B_{11}, B_{22}, B_{33}, B_{44}\big)$;

$C = \text{blockdiag}\big(C_{11}, C_{22}, C_{33}, C_{44}\big)$, A_{ii}, B_{ii} and C_{ii} are the same as A_i, B_{iu}, C_i as given in Eq. (18). The A_{ij} is given by:

$$A_{ij} = [a_{ij}]_{i=1,\ldots,n_i;j=1,\ldots,n_j}$$

where n_i and n_j are the number of state variables area i and j, respectively and for the given sample system n_1, n_2, n_3 and n_4 are 7. The all entries of A_{ij} is zero except the a_{21} is $-T_{ij}$.

A 4×4 transfer function matrix for the system can be obtained as $G(s) = C(sI - A)^{-1}B$. A Nyquist array with the row Gershgorin circles on the diagonal elements is plotted in Fig. 8. The frequency responses of the second diagonal element with the Gershgorin circles enclose the origin of the complex plane. This and an inverse Nyquist array (not plotted here) show that the system is not diagonal dominant. The P-F eigenvalues related to the $G(s)$ are depicted in Fig. 9 which shows that it is impossible to use a diagonal compensator to achieve the required diagonal dominance. It is therefore also not possible to use the Nyquist array method to design the required decentralized controller [17].

To break the limit imposed by the diagonal dominance, the design method proposed in this paper is applied here.

Simulation results and eigenvalue analysis show that the open loop system performance is affected more significantly by changing in the K_{pi}, T_{pi}, B_I and T_{jj} than changes of other parameters. Thus, to illustrate the capability of the proposed strategy in this example, in the view point of uncertainty our focus will be concentrated on variation of these parameters. Hence, for the given power system, we have set our objectives to area frequency regulation and assuring robust stability and performance in the presence of specified uncertainties, load changes and contract variations as follows:

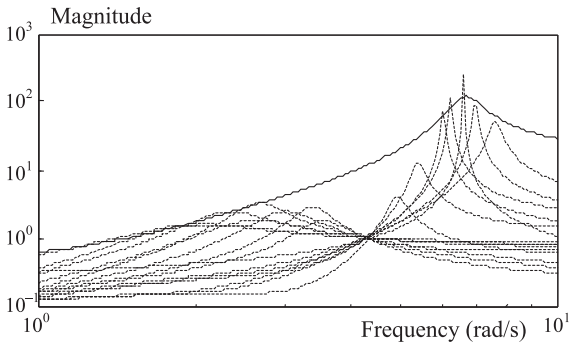

Fig. 10. Uncertainty plot due to change of K_{p1}, T_{p1}, B_1 and T_{j1} (dashed) and $W_{u1}(s)$ (solid).

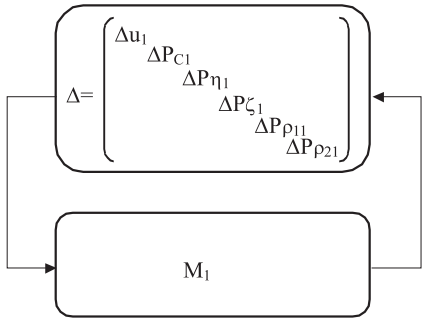

Fig. 11. Standard $M-\Delta$ block for area 1.

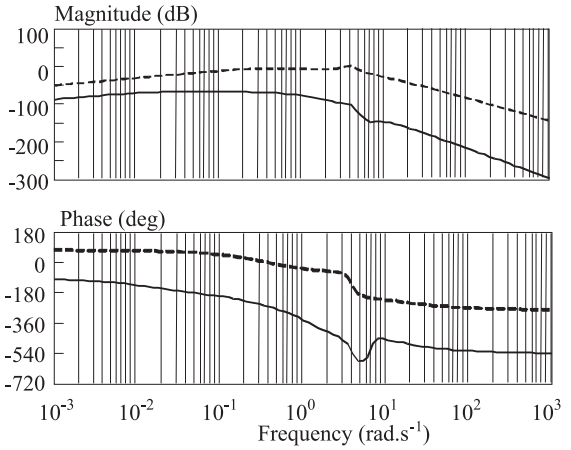

Fig. 12. Bode plot of $K_1(s)\tilde{G}_1(s)$ (solid) and $\tilde{G}_1(s)$ (dashed).

1. Holding stability and robust performance for the overall power system and each control area in the presence of 20 % uncertainty for the K_{pi}, T_{pi}, B_i and T_{ji}.
2. Minimizing the effects of new introduced disturbances on the output signals according to the possible contracts.
3. Getting zero steady state error and good tracking for load demands and disturbances.
4. Maintaining acceptable overshoot and settling time on the frequency deviation signal in each control area.
5. Setting the reasonable limit on the control action signal from the change speed and amplitude view point.

Following, we will discuss application of the proposed strategy on the given power system to achieve the above objectives for each of the four control areas separately. Because of similarity and to save space, the first controller synthesis will be described in detail and for the other control areas, only the final results will be presented.

Uncertainty weights selection: As it is mentioned in the previous section, we can consider the specified uncertainty in each area as a multiplicative uncertainty associated with a nominal model. Let $\hat{P}_i(s)$ denote the transfer function from the control input u_i to control output y_i at operating points other than the nominal point. Following a practice common in robust control, this transfer can be represented as:

$$\begin{aligned} &|\Delta u_i(s)W_i(s)| = \left|\left(\hat{P}_i(s) - P_{oi}(s)\right)/P_{oi}(s)\right|;\ P_{oi}(s) \neq 0 \\ &\|\Delta u_i(s)W_i(s)\|_\infty = \sup|\Delta_i(s)| \leq 1 \end{aligned} \tag{27}$$

where, $\Delta u_i(s)$ shows the uncertainty block corresponding to the uncertain parameters and $P_{oi}(s)$ is the nominal transfer function model. Thus, $W_{ui}(s)$ is such that its magnitude Bode plot covers the Bode plot of all possible plants. Using Eq. (27) some sample uncertainties corresponding to different values of K_{pi}, T_{pi}, B_i and T_{jj} are shown in Fig. 10 for one area. It can be seen that multiplicative uncertainties have a peak around the 6.5 rad/s. Based on this figure the following multiplicative uncertainty weight was chosen for control design as:

$$W_{u1} = \frac{16.13s^2 + 26.22s + 21.33}{s^2 + 0.9s + 44.07} \tag{28}$$

Figure 10 clearly shows that attempting to cover the sharp peak around the 6.5 rad/s will result in large gaps between the weight and uncertainty at other frequencies. On the other hand, a tighter fit at all frequencies using a high order transfer function will result in a high order controller. The weight (28) used in our design give a conservative design at around the 6.5 rad/s, low and high frequencies, but it provides a good trade off between robustness and controller complexity. Using the same method, the uncertainty weighting function for area 2, 3 and 4 are calculated as follows:

$$\begin{aligned} W_{u2} &= \frac{19.7s^3 + 17.32s^2 + 232.1s + 53.29}{s^3 + 4.49s^2 + 41s + 148.2} \\ W_{u3} &= \frac{68s^3 + 154.9s^2 + 41s + 148.2}{s^3 + 31.16s^2 + 84.7s + 1159} \\ W_{u4} &= \frac{16666s^3 + 3510s^2 + 31414s + 25311}{s^3 + 1150s^2 + 1364.1s + 36489} \end{aligned} \tag{29}$$

Performance weights selection: As we discussed in Sec. 4, in order to guarantee robust performance and satisfy the control objectives of AGC problem, we need to add for each of the control area a fictitious uncertainty block along with the corresponding performance weights W_{Ci} and W_{Pi} ($W_{\eta i}$, $W_{\zeta i}$, $W_{\rho 1i}$, $W_{\rho 2i}$) associated with the

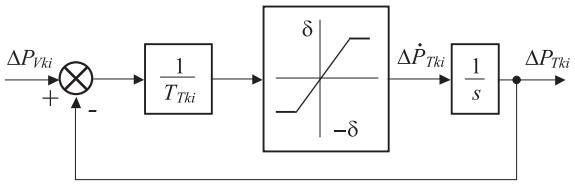

Fig. 13. A nonlinear turbine model with GRC.

Table 3. The set of weighting functions

Weight	Area-2	Area-3	Area-4
W_{Ci}	$\frac{0.05s}{0.0001s+1}$	$\frac{0.04s}{0.0001s+1}$	$\frac{0.04s}{0.0001s+1}$
$W_{\eta i}$	$\frac{0.12}{200}\frac{s+1}{s+0.01}$	$\frac{s+0.024}{40(s+0.01)}$	$\frac{s+0.05}{280(s+0.001)}$
$W_{\zeta i}$	$\frac{0.15}{200}\frac{s+5}{s+0.05}$	$\frac{s+0.075}{25(s+0.05)}$	$\frac{s+0.1}{120(s+0.005)}$
$W_{\rho 1i}$	$\frac{0.12}{350}\frac{s+0.6}{s+0.06}$	$\frac{0.5s+0.036}{350(0.5s+0.003)}$	$\frac{s+0.05}{130(s+0.003)}$
$W_{\rho 2i}$	$\frac{0.12}{190}\frac{s+0.4}{s+0.04}$	$\frac{0.1s+0.048}{190(0.1s0.004)}$	$\frac{s+0.05}{100(s+0.004)}$

Table 4. Gain and phase margins.

	$\widetilde{G}_i(s)$		$K_i(s)\widetilde{G}_i(s)$	
	GM (dB)	PM (deg)	GM (dB)	PM (deg)
Loop 1 (Area-1)	2.32	8.01	65.33	∞
Loop 2 (Area-2)	8.03	37.99	68.65	∞
Loop 3 (Area-3)	9.15	41.62	47.78	∞
Loop 4 (Area-4)	5.14	17.33	76.86	∞

control effort and control area error minimization, respectively. The selection of W_{Ci} and W_{Pi} entails a trade off among different performance requirements, particularly good regulation versus peak control action. The weight on the control input W_{Ci} must be chosen close to a differentiator to penalize fast change and large overshoot in the control input. The weight on the output error W_{Pi} must be close to an integrator at low frequencies in order to get zero steady state error, good tracking and disturbances rejection. On the other hand, an important issue in regard to selection of these weights is degree for achieving performance objectives. Moreover, in order to keep the controller complexity low, the order of selected weights should be kept low. More details on how these weights are chosen are given in [24, 25]. Based on the above discussion, a suitable set of performance weighting functions for one control area is chosen as:

$$W_{C1} = \frac{0.5s}{0.01s+1}, \quad W_{\eta 1} = \frac{0.12}{95}\frac{s+1}{s+0.01},$$
$$W_{\xi 1} = \frac{0.15}{120}\frac{s+5}{s+0.05}, \tag{30}$$
$$W_{\rho 11} = \frac{0.12}{90}\frac{s+0.6}{s+0.06}, \quad W_{\rho 12} = \frac{0.12}{110}\frac{s+4}{s+0.04}$$

Our next task is to isolate the uncertainties from the nominal area model and redraw the system in the standard M–Δ configuration as shown in Fig. 11. By using the uncertainty description and developed performance weights, we get an uncertainty structure Δ with a scalar block (corresponding to the uncertainty) and a 5×5 block (corresponding to the performance).

Now, due to synthesis methodology as given in Sec. 4, the robust synthesis problem is obtained in terms of the μ-theory, and the μ-analysis and synthesis toolbox is used to obtain optimal controller. The controller $K_1(s)$ is found at the end of the first D–K iteration, yielding the value of about 0.962 on the upper bound on μ. Thus, the robust performance is guaranteed. The resulting controller is a dynamic type and has a high order (15^{th}). The controller is reduced to a 4^{th} order with no performance degradation using the standard Henkel norm approximation. The transfer function of the reduced order controller is given by:

$$K_1(s) = 1.45\times 10^{-5}\frac{s^3 - 0.16s^2 + 25.37s + 9.15}{s^4 + 2.79s^3 + 4.65s^2 + 1.65s + 0.067} \tag{31}$$

Using the same procedure and setting similar objectives as discussed above the set of suitable weighting function for the other control area synthesizes are given in Table 3. The resulting controllers can be approximated by low order controllers as follows:

$$K_2(s) = 6.15 \times 10^{-5}\times$$
$$\frac{s^4 - 20.46s^3 + 7.19s^2 - 530.44s + 4.76}{s^5 + 21.3s^4 + 74.19s^3 + 316.05s^2 + 119.76s + 4.76}$$
$$K_3(s) = 1.4 \times 10^{-4}\times \tag{32}$$
$$\frac{s^5 - 6.49s^4 + 48.5s^3 + 241.1s^2 - 99.53s - 5.47}{s^6 + 6.64s^5 + 28.42s^4 + 103.83s^3 + 87.67s^2 + 17.09s + 0.529}$$
$$K_4(s) = -4.62 \times 10^{-6}\times$$
$$\frac{s^4 - 6.03s^3 + 44.54s^2 + 431.9s + 17.94}{s^5 + 12.20s^4 + 29.38s^3 + 33.06s^2 + 11.86s + 0.0078}$$

Using the above decentralized controllers and the formulae mentioned in Sec. 2 the IM defined before is obtained as: 26.6 dB. The frequency response of $K_1(s)\tilde{G}_1(s)$ and $\tilde{G}_1(s)$ are shown in Fig. 12. The GM is increased from 2.32 to 65.33 dB and the PM is increased from 8.01° to infinity. The improvements each individual loop's GM and PM are listed in Table 4 for all areas.

The above results show that when the frequency response based diagonal dominance cannot be achieved, the condition based on the H_∞ norm and structured singular value can be applied to design decentralized controller for the required system performance.

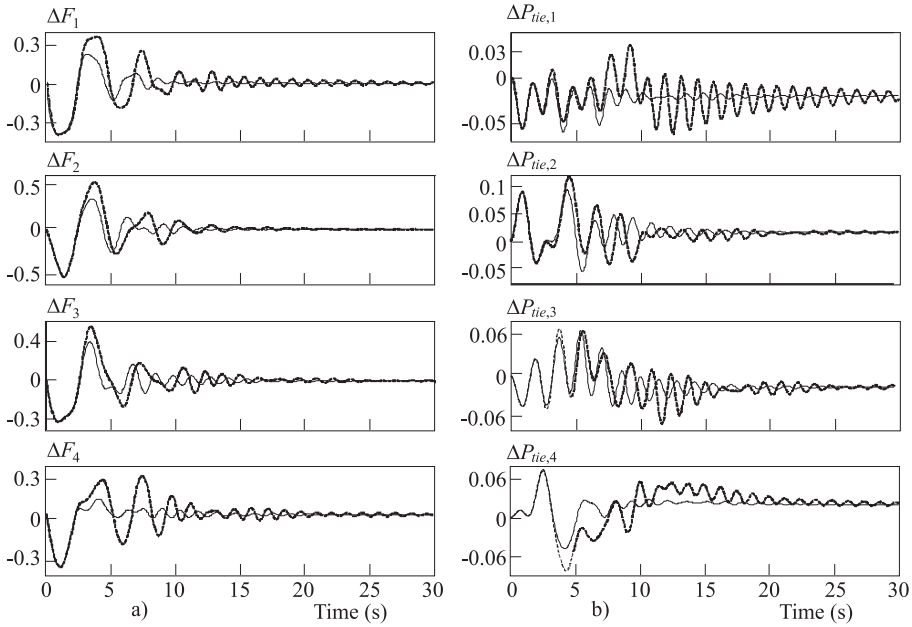

Fig. 14. Power system responses to scenario 1: a) Frequency deviation b) Tie line power changes; Solid (μ-based) and Dashed (PI).

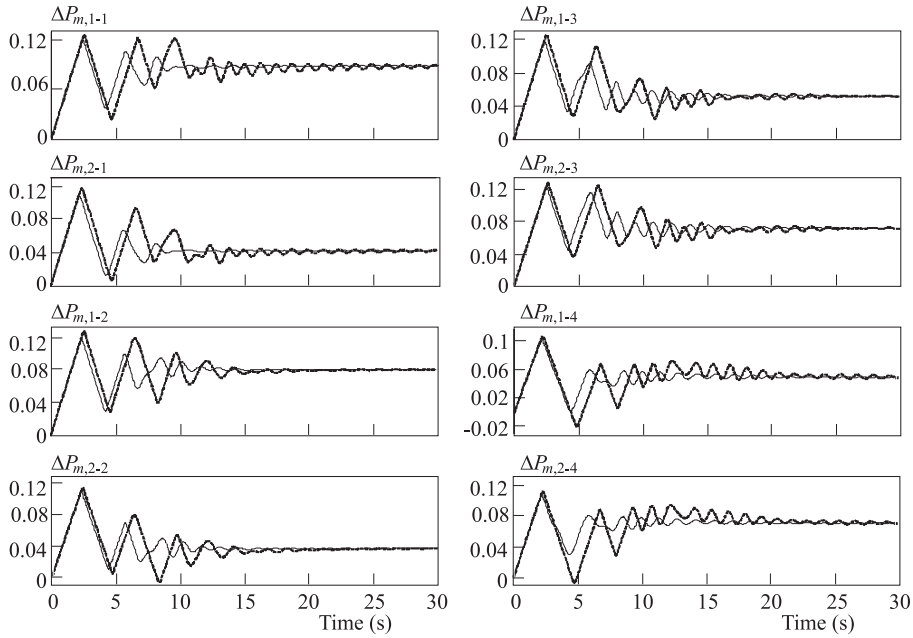

Fig. 15. GENCOs Power changes; Solid (μ-based) and Dashed (PI).

6 SIMULATION RESULTS

In order to illustrate the behaviour of the proposed control strategy some simulations has been carried out. In the simulation study, the linear model of a turbine $\Delta P_{VKi}/\Delta P_{TKi}$ in Fig. 3 for each GENCO is replaced by a nonlinear model of Fig. 13 (with ± 0.05 limits). This is to take GRC into account *ie* the practical limit on the area of change in the generating power of each GENCO. It is noted that GRC would influence the dynamic responses of the system significantly and lead to longer overshoot and longer settling time.

The close loop system performance using the proposed μ-based controllers in comparison with the conventional PI controllers (which is widely used for AGC problem in industry) is tested for two cases of operating conditions in the presences of load demands, disturbances and uncertainties.

6.1 Scenario 1

In this scenario, the closed loop performance is tested in the presence of both step contracted load demands and uncertainties. It is assumed that a large step load is

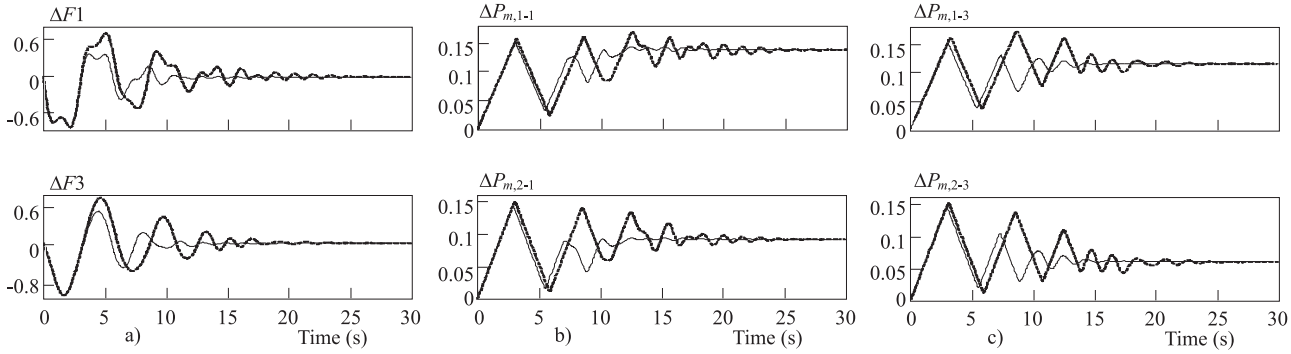

Fig. 16. a) Frequency deviation b) GENCOs Power changes in area 1 c) GENCOs Power changes in area 3, Solid (mu-based) and Dashed (PI).

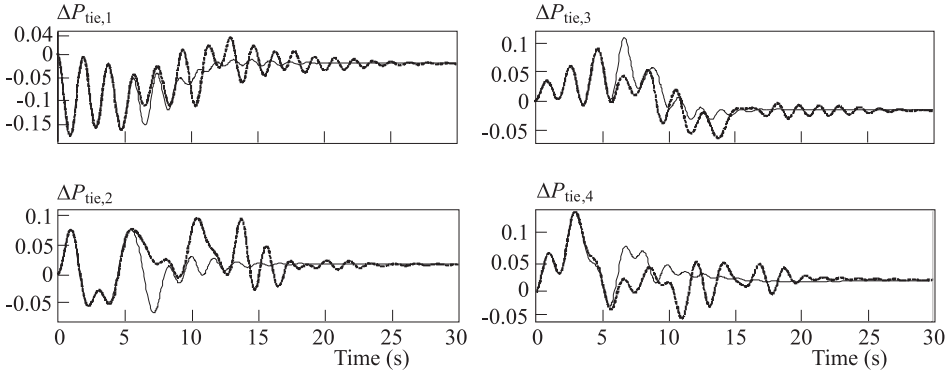

Fig. 17. a) Frequency deviation b) GENCOs Power changes in area 1 c) GENCOs Power changes in area 3, Solid (mu-based) and Dashed (PI).

demanded by all DISCOs as follow:

$$\Delta P_{L1\text{-}1} = 100\,, \quad \Delta P_{L2\text{-}1} = 50\,, \quad \Delta P_{L1\text{-}2} = 100\,, \text{MW}$$

$$\Delta P_{L1\text{-}3} = 80\,, \quad \Delta P_{L2\text{-}3} = 60\,, \quad \Delta P_{L1\text{-}4} = 100\,, \text{MW}$$

A case of combined Poolco and bilateral based contracts between DISCOs and available GENCOs is considered based on the following AGPM:

$$AGPM^{\top} = \begin{bmatrix} 0.4 & 0 & 0.4 & 0 & 0.2 & 0 & 0 & 0 \\ 0 & 0.2 & 0 & 0.4 & 0 & 0 & 0 & 0.4 \\ 0 & 0 & 0.4 & 0 & 0 & 0.6 & 0 & 0 \\ 0 & 0.4 & 0 & 0.2 & 0.4 & 0 & 0 & 0 \\ 0.8 & 0 & 0 & 0 & 0 & 0.2 & 0 & 0 \\ 0 & 0 & 0 & 0 & 0 & 0 & 0.5 & 0.5 \end{bmatrix}$$

All GENCOs participate in the AGC task. The one GENCO in area 4 only participate for performing the AGC in its area, while other GENCOs track the load demand in their areas and/or others. Power system responses with 20 % increase in uncertain parameters K_{Pi}, T_{Pi}, B_i and T_{ij} are depicted in Figs. 14 and 15. Using the proposed method, the frequency deviation of all areas is quickly driven back to zero and the tie-line power flows properly converges to the specified values of Eq. (13) in the steady state, *ie*:

$$\Delta P_{tie,1,sch} = -0.05\,, \quad \Delta P_{tie,2,sch} = 0.016\,\text{pu MW},$$
$$\Delta P_{tie,3,sch} = -0.016\,, \quad \Delta P_{tie,4,sch} = 0.02\,\text{pu MW},$$

Also, the actual generated powers of GENCOs properly reached the desired values in the steady state as given by Eq. (17), *ie*:

$$\Delta P_{m,1\text{-}1} = 0.088\,,\ \Delta P_{m,2\text{-}1} = 0.042\,,$$
$$\Delta P_{m,1\text{-}2} = 0.08\,,\ \Delta P_{m,2\text{-}2} = 0.036\,,\ \text{pu}$$
$$\Delta P_{m,1\text{-}3} = 0.052\,,\ \Delta P_{m,2\text{-}3} = 0.072\,,$$
$$\Delta P_{m,1\text{-}4} = 0.05\,,\ \Delta P_{m,2\text{-}4} = 0.07\,,\ \text{pu}$$

6.2 Scenario 2

In this case, a DISCO may violate a contract by demanding more power than that specified in the contract. This excess power is reflected as a local load of the area (un-contracted load). Consider scenario 1 again. It is assumed that in addition to specified contracted load demands and 20 % decrease in uncertain parameters, the one DISCO from areas 1 and 2 demand 0.1 and 0.05 pu MW as a large un-contracted load, respectively. Using the Eq. (10), the total local load in all areas is obtained as:

$$\Delta P_{LOC,1} = 0.25\,, \qquad \Delta P_{LOC,2} = 0.16\,\text{pu MW}$$
$$\Delta P_{LOC,3} = 0.14\,, \qquad \Delta P_{LOC,4} = 0.1\,\text{pu MW}$$

The purpose of this scenario is to test the effectiveness of the proposed controller against uncertainties and large

Table 5. ITAE values

Test No	Parameter Change (%)	Scenario 1 μ-Based	Scenario 1 PI	Scenario 2 μ-Based	Scenario 2 PI
0	0	256	481.2	1007.1	1975.8
1	+5	269.1	492.3	1248.3	2597.2
2	-5	245.7	396.8	833.5	2046.1
3	+10	271.7	604.2	1310.5	2946.1
4	-10	241.9	309.8	698.1	1493.1
5	+15	254.1	754.4	1281.7	2335.4
6	-15	233.9	263.6	562.4	1192.9
7	+20	222.6	955.1	1274	3344.1
8	-20	213.3	249.7	543.7	1113.1

Table 6. FD values

Test No	Parameter Change (%)	Scenario 1 μ-Based	Scenario 1 PI	Scenario 2 μ-Based	Scenario 2 PI
0	0	591.8	881.2	1864.4	2954.7
1	+5	618.4	864	2118.9	2978
2	-5	601.2	841.1	1667.1	2864.8
3	+10	605.8	944.3	2205.7	3006.5
4	-10	612.3	806.9	1386.2	2704.6
5	+15	550.8	1196.8	2240.1	2998.3
6	-15	617.1	808	1193.3	2364.4
7	+20	494.8	1411.5	2254.3	2935.7
8	-20	573.8	799.8	1053.6	2052.6

load disturbances in the presence of GRC. The power system responses for areas 1 and 2 are shown in Figs. 16 and 17. Using the proposed method, the frequency deviation of these areas is quickly driven back to zero and the tie-line power flows properly converge to the specified value of Eq. (14) in the steady state. As AGPM is the same as in scenario 1 and the un-contracted load of areas is taken up by the GENCOs in the same areas, the tie-line power is the same as in scenario 1 in the steady state (Fig. 16).

The un-contracted load of DISCOs in area 1 and 2 is taken up by the GENCOs in these areas according to ACE participation factors in the steady state. Using the Eq. (17) the actual generated power of GENCOs in above areas is given by:

$$\Delta P_{m,1\text{-}1} = 0.138\,, \qquad \Delta P_{m,2\text{-}1} = 0.092\,\text{pu MW}$$
$$\Delta P_{m,1\text{-}2} = 0.116\,, \qquad \Delta P_{m,2\text{-}3} = 0.06\,\text{pu MW}$$

As shown in Figs. 16-b and c, the actual generated powers of GENCOs properly reached the desired values using the proposed strategy.

The simulation results in the above scenarios indicate that the proposed control strategy can ensure the robust performance such as frequency tracking and disturbance attenuation for possible contracted scenarios under modelling uncertainties and large area load demands in the presence of GRC. To demonstrate robust performance of the proposed control strategy, the performance indices Integration-Time-Absolute-Error (ITAE) based on ACE and Figure of Demerit (FD) based on system performance characteristics (suitably weighted) is being used as:

$$ITAE = 100 \int_0^{30} |ACE_1(t)|t\,\mathrm{d}t$$
$$FD = (OS \times 50)^2 + (US \times 30)^2 + T_S^2$$

Overshoot (OS), undershoot (US) and settling time (for 5 % band of the total step load demand in area 1) of frequency deviation area 1 are considered for evaluation of FD. The numerical results of the performance robustness for two above scenarios under different uncertainty system parameters changes are listed in Tables 5 and 6. Examination of these Tables reveals that in comparison with PI controllers, the system performance is significantly improved by the controllers designed in this paper; and this control strategy is robust against the plant parameter changes.

7 CONCLUSION

A new decentralized robust load frequency controller in the deregulated power system using the generalized AGC scheme model for accounting the effects of the possible load following contracts is proposed in this paper. It is shown that, when the frequency response based diagonal dominance can not be achieved, subject to a condition based on the H_∞ norm and structured singular values (μ), each local area controller can be designed independently. Since, each control area contains different kinds of uncertainties and disturbances in the deregulated power system the idea of μ-synthesis technique have been used to solve the AGC problem. This control strategy was chosen because of the flexibility of the synthesis procedure to modelling uncertainties, setting the desired level of the robust performance and considering practical constrains by introducing appropriate uncertainties. The proposed method leads to a set of relatively simple controllers which is ideally practical for the real world complex power systems.

The effectiveness of the proposed control strategy was tested on a multi-area power system for a wide range of operating conditions in comparison with the conventional PI controller. The simulation results show that the proposed μ-based controller is superior to PI controller and achieve good robust performance such as frequency regulation, tracking the load demands and disturbances attenuation under a wide range of plant parameter change and area-load conditions. The system performance characteristics in terms of ITAE and FD indices reveal that the proposed method is a promising control scheme to solve the AGC problem in a competitive electricity environment.

Appendix A: Nomenclature

F	area frequency
P_{Tie}	net tie-line power flow turbine power
P_V	governor valve position
P_C	governor set point
ACE	area control error
apf	ACE participation factor
Δ	deviation from nominal value
K_P	subsystem equivalent gain
T_P	subsystem equivalent time constant
T_T	turbine time constant
T_H	governor time constant
R	droop characteristic
B	frequency bias
K	gain of integral controller
T_{ij}	tie line synchronizing coefficient between area i and j
P_{Lj}	contracted demand of Disco j
P_{ULj}	uncontracted demand of Disco j
$P_{m,ji}$	power generation of GENCO j in area i
P_{Loc}	total local demand
η	area interface
ζ	scheduled power tie line power flow deviation

References

[1] JALEELI, N.—Van SLYCK, L. S.—EWART, D. N.—FINK, L. H.—HOFFMANN, A. G.: Understanding Automatic Generation Control, IEEE Trans. on Power Systems **7** (3) (1992), 1106–1122.

[2] RAINERI, R.—RIOS, S.—SCHIELE, D.: Technical and Economic Aspects of Ancillary Services Markets in the Electric Power Industry: an International Comparison, Energy Policy (2005), in press.

[3] DONDE, V.—PAI, A.—HISKENS, I. A.: Simulation and Optimization in a AGC System after Deregulation, IEEE Trans. on Power Systems **16** (3) (2003), 481–489.

[4] KUMAR, J.—HOE, N. G.—SHEBLE, G.: AGC Simulator for Price-Based Operation. Part I: Modelling, IEEE Trans. on Power Systems **12** (2) (1997), 527–532.

[5] CHRISTIE, R. D.—BOSE, A.: Load Frequency Control Issues in Power System Operations after Deregulation, IEEE Trans. on Power Systems **11** (3) (1996), 1191–1200.

[6] SHAYANFAR, H. A.—SHAYEGHI, H.: Decentralized Load Frequency Control of a Deregulated Electric Power System Using ANN Technique, WSEAS Trans. on Circuits and Systems **4** (1) (2005), 38–47.

[7] ARROYO, J. M.—CONEJO, A. J.: Optimal Response of a Power Generator to Energy, AGC and Reserve Pool-Based Markets, IEEE Trans. on Power Systems **17** (2) (2002), 404–410.

[8] BAKKEN, B. H.—GRANDE, O. S.: Automatic Generation Control in a Deregulated Power System, IEEE Trans. on Power Systems **13** (4) (1998), 1401–1406.

[9] MELIOPOULOS, A. S.—COKKINIDES, G. J.—BAKIRTZIS, A. G.: Load Frequency Control in a Deregulated Environment, Decision Support Systems **24** (1999), 243–50.

[10] LIU, F.—SONG, Y. H.—MA, J.—LU, Q.: Optimal Load Frequency Control in Restructured Power Systems, IEE Proc. on Gener. Transm. Distrib. **150** (1) (2003), 87–95.

[11] RERKPREEDAPONG, D.—HASANOVIC, A.—FELIACHI, A.: Robust Load Frequency Control Using Genetic Algorithms and Linear Matrix Inequalities, IEEE Trans. on Power Systems **18** (2) (2003), 855–861.

[12] FELIACHI, A.: On Load Frequency Control in a Deregulated Environment, IEEE Inter. Conf. on Control Applications (1996), 437–441.

[13] BEVRANI, H.—MITANI, Y.—TSUJI, K.: Robust Decentralized AGC in a Restructured Power System, Energy Conversion and Management **45** (2004), 2297–2312.

[14] ROSENBROCK, H. H.: Computer Aided Control System Design, Academic Press, 1974.

[15] MUMRO, N.: Recent Extensions to the Inverse Nyquist Array Design Method, Proc. 24$^{\text{th}}$ CDC Conf., 1985, pp. 1852–1857.

[16] MUMRO, N.—EDMUNDS, J. M.: The Inverse Nyquist Array and Characteristic Locus Design Methods, In: The Control Handbook (Levine W.S., ed.), CRC/IEEE Press, 1996.

[17] MEES, A. I.: Achieving Diagonal Dominance, Systems and Control Letters **1** (1981), 155–158.

[18] LABIBI, B.—LOHMANN, B.—KHAKI SEDEGH, A.—JABEDAR MARALANI, P.: Output Feedback Decentralized Control of Large-Scale Systems Using Weighted Sensitivity Functions Minimization, Systems and Control Letters **47** (2002), 191–198.

[19] GROSDIDIER, P.—MORARI, M.: Interaction Measures for System under Decentralized Control, Automatica **22** (3) (1986), 309–319.

[20] SHAYEGHI, H.—SHAYANFAR, H. A.: Decentralized Robust Load Frequency Control Using Linear Matrix Inequalities in a Deregulated Multi-Area Power System, Journal of Power Engineering Problems No. 2 (2005), 30–38.

[21] ZHOU, K.—DOYLE, J. C.—GLOVER, K.: Robust and Optimal Control, Prentice Hall, 1996.

[22] DJUKANOVIC, M. B.—KHAMMASH, M. H.—VITTAL, V.: Sensitivity Based Structured Singular Value Approach to Stability Robustness of Power Systems, IEEE Trans. on Power Systems **15** (2) (2000), 825–830.

[23] BALAS, G. J.—DOYLE, J. C.—GLOVER, K.—PACKARD, A.—SMITH, R.: The μ-Analysis and Synthesis Toolbox for Use with MATLAB, The Mathworks Inc., South Natick, 1998.

[24] SKOGESTED, S.—POSTLETHWAITE, I.: Multivariable Feedback Control, John Wiley & Sons, 1996, pp. 449–467.

[25] SHAYEGHI, H.—KARRARI, M.: Theory of μ Synthesis for Power Systems Load Frequency Control, Journal of Electrical Engineering **51** (2000), 258–263.

Received 12 September 2005

Hossein Shayeghi received the BS and MSE degrees in electrical engineering from KNT and Amirkabir Universities of Technology in 1996 and 1998, respectively and the PhD degree in Electrical Engineering from Iran University of Science and Technology (IUST), Tehran, Iran, in 2006. Currently, he is an Assistant Professor at Technical Engineering Department of The University of Mohaghegh Ardebili, Ardebil, Iran. His research interests are in the application of robust control, artificial intelligence to power system control design and power system restructuring. He is a member of the Iranian Association of Electrical and Electronic Engineers (IAEEE) and a member of IEEE.

Heidar Ali Shayanfar received the BS and MSE degrees in electrical engineering in 1973 and 1979 and the PhD degree in electrical engineering from Michigan State University, USA, in 1981. Currently, he is a full professor at Electrical Engineering Department of IUST, Tehran, Iran. His research interests are in the application of artificial intelligence to power system control design, dynamic load modelling, power system observability studies and voltage collapse. He is a member of the Iranian Association of Electrical and Electronic Engineers (IAEEE) and IEEE.